PARTICULATE MATTER EMISSIONS FOR DUST FROM UNIQUE MILITARY ACTIVITIES

Dr. J.A. Gillies, Dr. V. Etyemezian, Dr. H. Kuhns,
Dr. H. Moosmüller, Dr. J. Engelbrecht, Dr. J. King, Mr. S. Uppapalli,
Mr. G. Nikolich, Mr. J.D. McAlpine, and Dr. D.A. Gillette

Dr. K.J. Allwine

Annual Report for SERDP Project SI-1399

Prepared for:

Mr. Bradley Smith
and
Dr. John Hall

December 31, 2007

Report Documentation Page

Form Approved
OMB No. 0704-0188

1. REPORT DATE	2. REPORT TYPE	3. DATES COVERED
31 DEC 2007		**00-00-2007 to 00-00-2007**

4. TITLE AND SUBTITLE	5a. CONTRACT NUMBER
Particulate Matter Emissions for Dust From Unique Military Activities	5b. GRANT NUMBER
	5c. PROGRAM ELEMENT NUMBER
6. AUTHOR(S)	5d. PROJECT NUMBER
	5e. TASK NUMBER
	5f. WORK UNIT NUMBER
7. PERFORMING ORGANIZATION NAME(S) AND ADDRESS(ES) **Strategic Environmental Research and Development (SERDP),Arlington,VA,22203-1821**	8. PERFORMING ORGANIZATION REPORT NUMBER
9. SPONSORING/MONITORING AGENCY NAME(S) AND ADDRESS(ES)	10. SPONSOR/MONITOR'S ACRONYM(S)
	11. SPONSOR/MONITOR'S REPORT NUMBER(S)

12. DISTRIBUTION/AVAILABILITY STATEMENT
Approved for public release; distribution unlimited

13. SUPPLEMENTARY NOTES

14. ABSTRACT

15. SUBJECT TERMS

16. SECURITY CLASSIFICATION OF:			17. LIMITATION OF ABSTRACT	18. NUMBER OF PAGES	19a. NAME OF RESPONSIBLE PERSON
a. REPORT	b. ABSTRACT	c. THIS PAGE			
unclassified	**unclassified**	**unclassified**	**Same as Report (SAR)**	**32**	

TABLE OF CONTENTS

LIST of TABLES

LIST of FIGURES

ACKNOWLEDGEMENTS

The SI-1399 research team would like to acknowledge the SERDP, Sustainable Infrastructure program for their sponsorship. The team would also like to thank the US Army Yuma Proving Ground, Yuma AZ, and specifically the Natural Events Test Office for their aid in coordinating our measurement activities with rotary-winged aircraft.

1. BACKGROUND

Particulate Matter (PM) emission is a critical problem for the Department of Defense (DoD). PM emitted during DoD testing and training activities threatens the safety and respiratory health of military personnel and can impact the health of urban populations encroaching on military installations. Moreover, new regulations protecting visibility at Class I national parks, forests, and wilderness areas mandate reductions in PM emissions and its chemical precursors over the next 60 years. Since many military installations are located near Class I areas, these regulations are likely to affect training activities in coming years. Military activities create unique dust emission sources not encountered in the civilian environment and which have not been accurately characterized and quantified. Without source specific emissions factors of known precision and accuracy, the uncertainties on these estimates are high. Understanding of the atmospheric and surficial influences on the amount of the dust available for longer distance transport as well as the modeling of this phenomenon remains poor. As a result emission factors applied without proper consideration of the factors that control the transportable fraction of PM will produce overestimates of these contributions.

2. OBJECTIVES

The objectives of this proposed research program are: 1) carry out field measurement campaigns to quantify dust emissions and develop emission factors for tracked military vehicles, rotary-winged aircraft, and artillery pieces for various unpaved surfaces, while extending our understanding of the important vehicle, activity, and surface characteristics that influence the magnitude of the observed emissions, 2) carry out measurement campaigns using the DRI flux tower system along with the ERDC-CERL team, which utilize remote-sensing measurements to develop emission factors of artillery backblast, tracked vehicles, and rotary-winged aircraft, 3) carry out limited measurements of dust emissions by fixed-wing aircraft in support ERDC-CERLs development of emission factor relationship for this dust source, 4) link the measured emission factors with indices of surface dust emission potential using a new portable wind tunnel and an on-vehicle measurement system thereby creating a cost effective mechanism to extend the use of the emission factors into different environments, 5) continue to develop a database from field and laboratory measurements that characterize the chemical, physical, and optical properties of the dust emissions that are important for assessing source contribution estimates and impacts on regional visibility degradation, 6) further develop a Geographic Information System-based dust dispersion modeling system that integrates the newly-developed emission factors into its user interface, 7) to disseminate the information, methods, and modeling products, generated from this research, to the military and civilian user community to improve their abilities to gather information, make decisions based on that information, and develop cost-effective solutions that will enhance military preparedness.

3. TECHNICAL APPROACH

The Desert Research Institute (DRI) and its research partners at the National Oceanic and Atmospheric Administration (NOAA), and Pacific Northwest National Laboratory

(PNNL) are conducting a systematic, empirically-based research program that combines environmental monitoring and controlled field experimentation to quantify and characterize dust emissions from unique DoD training and operational activities. DRI is utilizing flux tower measurement system and a downwind measurement method to quantify the emissions of PM generated by the different unique source types. In order to characterize the chemical properties of the emissions, samples of the emitted particulates are being collected on filters for laboratory analyses. State-of-the-art instruments to measure *in situ* the light scattering associated with the emitted particles is also being carried out during field campaigns.

This research will generate location-specific emission factors, but it will also seek to establish relationships between emission strengths and vehicle and surface characteristics that allow for their use at other installations. In addition we propose to utilize the Testing Re-entrained Aerosol Kinetic Emissions from Roads (TRAKER) system that quantifies dust emissions from paved and unpaved surfaces. TRAKER can be used to estimate emissions in different locations for different vehicle types because the ratio between TRAKER emissions and other vehicle types is established through field-testing comparisons. TRAKER can also be used to provide an index of dust emission potential for surfaces.

A new instrument system, the Portable In-Situ Wind ERosion Laboratory (PI-SWERL), developed at DRI to provide data on emission potential is also being used for this project. This small portable wind tunnel is used to develop an index that characterizes a surface's propensity to emit dust. By relating this index of emission potential for the test sites with measured emission factors derived from the environmental monitoring, emission potentials at different sites for different sources can be inferred using the cost effective PI-SWERL method.

In collaboration with PNNL we are also advancing the PNNL-developed GIS-based dust dispersion modeling system, DUSTRAN, (DUST TRANsport; SERDP project CP-1195) to incorporate the emissions factors derived from the measurements to simulate impacts on local and regional particulate air quality.

4. PROJECT ACCOMPLISHMENTS

4.1 DUST EMISSIONS FROM ARTILLERY BACKBLAST

The manuscript submitted in December 2006 describing emission of PM from artillery backblast was published in 2007. The full citation and abstract follow:

Gillies, J.A., V. Etyemezian, H. Kuhns, J. Engelbrecht, S. Uppapalli, and G. Nikolich (2007). Dust emissions caused by backblast from Department of Defense artillery testing. *Journal of the Air & Waste Management Association* **57**, doi:10.3155/1047-3289.57.5.551, 551–560.

There is a dearth of information on dust emissions from sources that are unique to the U.S. Department of Defense testing and training activities. However, accurate emissions factors are needed for these sources so that military installations can prepare accurate PM emission inventories. One such source, PM_{10} and $PM_{2.5}$ emissions from artillery backblast testing on improved gun positions, was characterized at the Yuma Proving Ground near Yuma, Arizona, in October 2005. Fugitive emissions are created by the

shockwave from artillery pieces, which ejects dust from the surface on which the artillery is resting. Other contributions of PM can be attributed to the combustion of the propellants. For a 155 mm howitzer firing a range of propellant charges or zones, amounts of emitted PM_{10} ranged from approximately 19 g-PM_{10} per firing event for a zone 1 charge to 92 g-PM_{10} per firing event for a zone 5. The corresponding rates for $PM_{2.5}$ were approximately 9 g-$PM_{2.5}$ and 49 g-$PM_{2.5}$ per firing. The average measured emission rates for PM_{10} and $PM_{2.5}$ appear to scale with the zone charge value. The measurements show that the estimated annual contributions of PM_{10} (52.2 metric tons) and $PM_{2.5}$ (28.5 metric tons) from artillery backblast are insignificant in the context of the 2002 U.S. EPA PM emission inventory. Using national-level activity data for artillery fire, the most conservative estimate is that backblast would contribute the equivalent of 5×10^{-4} % and 1.6×10^{-3} % of the annual total PM_{10} and $PM_{2.5}$ fugitive dust contributions, respectively, based on 2002 U.S. EPA inventory data.

4.2 DUST EMISSIONS FROM TRACKED VEHICLES

In FY06 a field campaign to measure dust emissions from tracked vehicles was carried out at the Yakima Test Center (YTC), Yakima WA, in October 2006. A second role for SI-1399 was to collect data in support of the remote sensing measurements made by SI-1400. The testing was undertaken with the cooperation of the YTC and the Washington State National Guard MATES Facility.

Based upon research findings presented by SI-1399 and SI-1400 it was decided in 2007 that it will be necessary to carry out a new series of tracked vehicle dust emission measurements in 2008. The data from the measurements made at YTC will be combined with the new measurements in 2008 to provide a more complete analysis of the range of emissions from tracked vehicles and evaluate how much of an influence soil type has on the strength of these emissions.

4.3 DUST EMISSIONS FROM ROTARY-WINGED AIRCRAFT

Measurements of dust emissions caused by a rotary-winged aircraft (UH-1H Huey) traveling over desert surfaces were made 21-25 May, 2007 at the Yuma Proving Ground, Yuma, AZ (Figure 1). The purpose of these measurements was to obtain data on the strength of dust emissions from desert surfaces caused by low level helicopter flight (~8 m for rotor height) for a range of speeds (15 km hr^{-1} – 60 km hr^{-1}), landing and take-off, and hovering (~12 m and ~20 m). Additional data were acquired to measure the vertical and horizontal wind speeds (m s^{-1}) in the zone directly under the flight path, and the surface shear stress (N m^{-2}) created by the rotor downwash as it moves laterally from the flight path. These data will also be used in concert with the remote sensing data collected by SERDP SI-1400 to develop rotary-winged aircraft dust emission factors.

The dust emission and environmental data collected during the May 2007 field campaign will also be used by the DRI Desert Terrain Project (an Army Research Office sponsored project) to test and validate a mechanistic helicopter dust emission model being developed as part of their research objectives. The Desert Terrain group will, as part of their research, extend the PI-SWERL measurements to other desert surfaces at the YPG to extrapolate the dust emission results to different desert surface conditions.

Figure 1. The YPG UH-1H Huey beginning a test pass along the defined flight line for the Roadrunner Drop Zone site.

The dust emission characterization measurements were accomplished through the interaction of research teams supported by SERDP, and the ARO-sponsored DRI Desert Terrain Forecasting group. Critical financial support that allowed these measurements to be obtained was provided by SERDP and the Natural Environments Test Office, YPG.

4.3.1 Rotary-Winged Aircraft Measurement Methodology

Dust emissions, surface shear stress, and surface wind measurements created by the YPG, UH-1H Huey were made at two different locations at the YPG, which represented two different desert surface types. This will allow us to compare and contrast the strength of the emissions from the same helicopter operating conditions (traversing the surface at low levels, take-off, landing, and hovering) between two sites with different dust emission potential.

The two sites at which measurements occurred are identified as the Roadrunner and Sidewinder Drop Zones. The first site, i.e. Roadrunner, represents a desert pavement surface. This type of surface is typical in some deserts and is characterized by a surface armoring of clasts that form a stable surface. The second site, i.e., Sidewinder, represents a disturbed desert soil surface that can be identified as a desert wash surface.

At each site a flight corridor was marked with traffic cones and sandbags to define a flight path for the helicopter (Figure 2). This flight corridor was approximately 100 m long. The instruments were placed on the expected downwind side to measure the emitted dust plumes that would be carried by the ambient winds. For this testing it was

expected that the scale of the rotary-winged created dust plumes would be considerably greater than could effectively be captured by the DRI flux tower (Gillies et al., 2005; Gillies et al., 2007) system supported by SERDP Project SI-1399. In order to overcome this limitation a second set of dust emission measurements were carried out with the optical remote sensing system of SERDP Project SI-1400 (ERDC-CERL, UIUC, & Arcadis), which consists of a micro-pulse lidar and two Fourier Transform Infrared Spectrometers (FTIR).

The three instrumented towers that comprise the DRI flux tower system were located along a plane, coincident with the remote sensing beams, within just several meters of distance (Figure 2). This allows us to provide dust mass concentration measurements with mass concentrations inferred from inversion of the lidar and FTIR signals. By capturing the mass of PM passing the flux plane the dust emissions resulting from the helicopter activity can be quantified.

As part of this campaign and prior to the dust emission measurements we used the DRI PI-SWERL system to characterize the dust emission potential of each surface. These measurements of emission potential will allow us to evaluate the relationship between measurements of emissions and the PI-SWERL dust emission index. The PI-SWERL measurements are discussed in a later section.

Figure 2. The instrumentation set up to measure dust emissions generated by the helicopter. The three visible towers comprise the DRI flux tower system and the optical remote sensing instruments (FTIR) are located by the panel truck. Their infrared beams are aimed at retro-reflectors on the scissor jack. The micropulse lidar is visible behind the scissor jack.

Along with the measurements of the magnitude of the dust emissions, SI-1399 also collected 3-dimensional wind speed data generated by the rotor-wash using a sonic anemometer deployed in the flight corridor. Multiple passes were made by the helicopter directly over the instrument as well as passes that were shifted one and two rotor diameters from the position of the sonic anemometer. Four Irwin sensors (Irwin, 1980), which have been previously used to measure surface shear generated by atmospheric boundary-layer winds (Gillies et al., 2006; Gillies et al., 2007) were embedded in the surface along an 18 m long transect normal to the flight path, beginning at a location 10 m from the center of the flight line. The four Irwin sensors were separated in decreasing distance from the edge of where the rotor-wash was expected to become directed laterally (i.e., 10 m, 5, m, 2.5 m, and 1.25 m) and sweep across the surface creating a horizontal shear stress. The purpose of these measurements is to relate helicopter operating conditions with the surface winds and turbulence they generate and the associated dust emission strength. Helicopter operating conditions were tabulated by the flight crew during operations and delivered to SI-1399 upon completion of each day's tests.

The testing at YPG consisted of the following:

Site 1: 33 helicopter passes with the rotor at ~8 m above the ground surface spanning the speed range 15 km hr^{-1} to 60 km hr^{-1}. In addition, four landing/takeoff maneuvers were executed directly in-line with the sonic anemometer and Irwin sensors.

Site 2: Our first attempt at measurements at this site on 05-23-07 was hampered by very poor wind conditions. Twenty passes were made, but most did not result in reasonable data. It was decided that for our last two hours of helicopter time we would stay at this location and try again on 05-25-07. On that day we had 37 helicopter passes down the designated flight line covering the speed range 15 km hr^{-1} to 60 km hr^{-1}, with the rotor height at ~8 m above the ground. In addition we measured dust emissions and rotor wash strength (sonic anemometer and Irwin sensors) for a 20 second hovering maneuver at ~15 m and ~7.5 m above ground level.

In addition to the real-time measurement of dust concentrations, integrated filter samples of the airborne dust created by the helicopter flights were collected and have been submitted for chemical analyses. Bulk soil samples were also collected for chemical and mineralogical analyses as well as for carrying out the calibrations of the DustTraks using the resuspension chamber method (Chow et al., 1994).

4.3.2 Results: Rotary-Winged Aircraft Dust Emissions

4.3.2.1 Dust Emissions

The dust emission measurements presented in this report represent (at this time) only data collected using the DRI flux tower system. However, the scaling relationships observed will be independent of the absolute values of the emissions, which will become available as the teams merge their data sets.

An example of the PM_{10} concentration data collected during the series of flights on May 25, 2007 are shown in Figure 3.

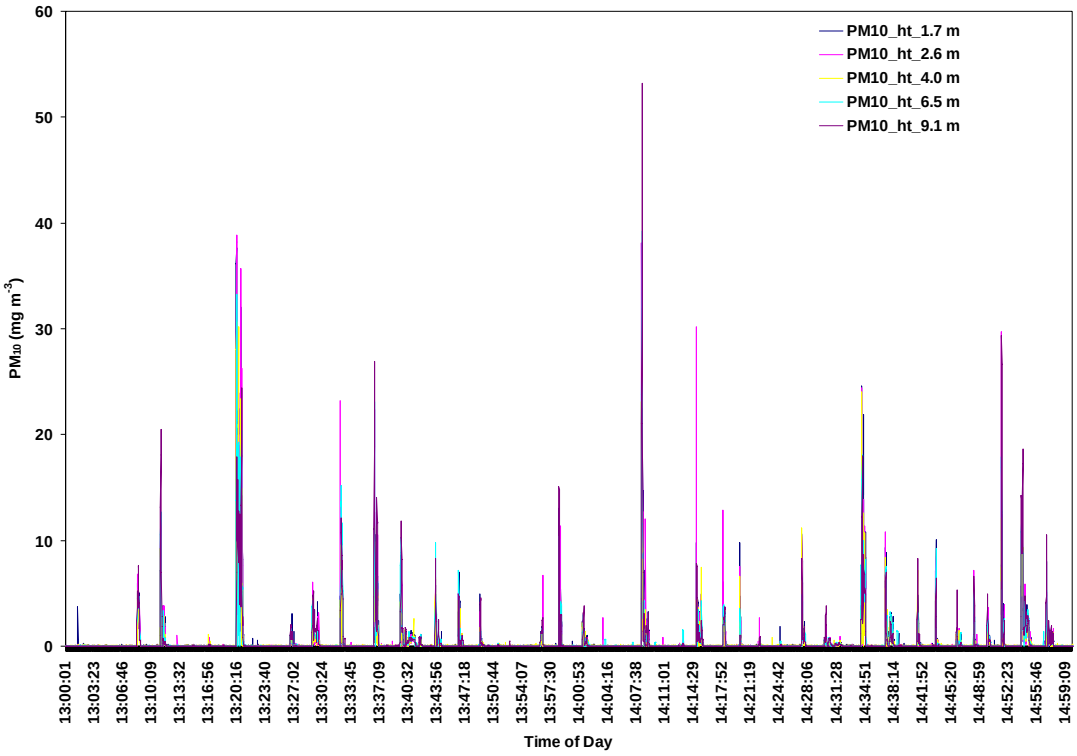

Figure 3. The PM_{10} dust concentrations measured for the helicopter passes made on May 25, 2007.

At this time we have identified all the periods of elevated dust concentrations that represent the emissions created by the helicopter passes. Of the total number of passes made (82) reliable data were obtained for 58, which represents a data recovery of 63%. Reasons for a failure to observe the emissions were a result of variable winds that caused the plume to miss the instrument array, or because winds dropped to near zero speed creating a plume that dispersed mostly due to thermal instabilities, which is not amenable to a standard horizontal flux calculation.

The duration that the helicopter-generated plumes impacted the towers ranged from 7 to 107 seconds at site 1, and 13 to 180 seconds at site 2. These times depend primarily on wind speed and wind direction, but are an important component of the flux calculation.

Peak concentrations of $PM_{2.5}$ measured (with the DustTrak sensors) at the towers associated with the dust plumes ranged from 1.285 mg m^{-3} to 9.925 mg m^{-3} at site one. Peak concentrations of PM_{10} at site one ranged from 6.046 mg m^{-3} to 38.860 mg m^{-3}. Background ambient concentrations between helicopter passes ranged between 0.024 mg m^{-3} and 0.108 mg m^{-3} for $PM_{2.5}$ and between 0.055 mg m^{-3} and 0.499 mg m^{-3} for PM_{10}.

At site 2, peak concentrations of $PM_{2.5}$ measured at the towers associated with the dust plumes ranged from 5.874 mg m^{-3} to 9.24 mg m^{-3}. Peak concentrations of PM_{10} at site two ranged from 33.147 mg m^{-3} to 53.170 mg m^{-3}. Background ambient concentrations between helicopter passes ranged between 0.019 mg m^{-3} and 0.139 mg m^{-3} $PM_{2.5}$ and between 0.040 mg m^{-3} and 0.205 mg m^{-3} for PM_{10}. These represent average 15 second concentrations (measured at 1 Hz) prior to the arrival of dust plumes.

The one second dust concentration data collected at each of the three towers at multiple heights can be combined with the wind speed and direction data to provide an estimate of how much dust passed through the tower-defined flux plane for each dust plume raised by the helicopter traveling down the flight line. It should be noted that the actual amount of dust will be higher because the defined flux plane does not capture the complete plume. It will be necessary to use the plume mapping capability of SI-1400 to estimate the actual scale of the generated plume and extrapolate the amount of dust in the entire plume as it passes the defined flux plane. A first estimate of how many kilograms of dust are passing by the flux plane as a function of forward travel speed of the helicopter are provided in Table 1. Clearly, site 2 the disturbed desert soil generates much higher dust emissions for the same helicopter traveling above the ground at the same height and over a similar range of speeds. For the same forward travel speeds of 15 km hr^{-1} and ~30 km hr^{-1} the emissions increase at site 2 by approximately 54 times. For the 60 km hr^{-1} speeds the emissions are approximately equivalent, suggesting forward travel speed greatly affects emission strength.

Although the absolute values of flux are not representative of the actual size of the emitted dust plumes these data allow us to examine scaling relationships between the operating condition of the helicopter and the dust emissions. The effect of forward travel speed on emissions can be demonstrated in Figure 4, which shows the average tower emission flux versus forward travel speed of the aircraft. This Figure clearly demonstrates the non-linear nature of the relationship. At both sites there is an exponential decrease in emission flux as a function of aircraft speed.

Table 1. Average flux of PM_{10} through the flux plane at each of the DRI flux-towers for each helicopter forward travel speed.

Site	Forward Travel Speed (km hr^{-1})	Average Per Tower Total Flux (kg of PM_{10} /flight pass)	Standard Deviation of Total Flux (kg of PM_{10} /flight pass)	Number of Flight Passes
1	15	0.294	0.351	14
1	30	0.098	0.137	13
1	60	0.065	0.059	15
2	15	15.156	10.762	27
2	25	6.202	6.062	24
2	35	4.496	3.942	25
2	45	0.708	0.802	28
2	60	0.071	0.064	3

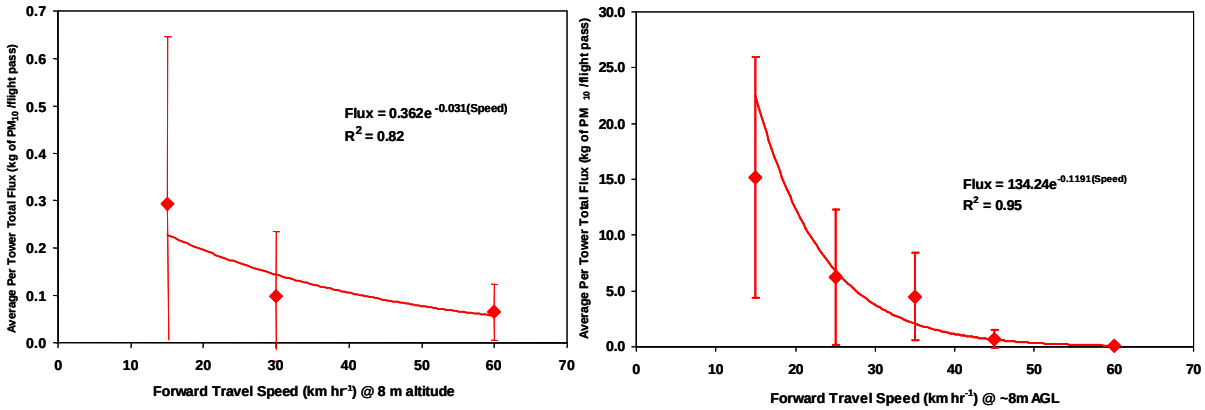

Figure 4. The decrease in PM_{10} dust flux as a function of helicopter forward travel speed for sites 1 (left) and 2 (right).

Normalizing the emission flux by dividing each mean flux at each travel speed by the mean flux for the 15 km hr^{-1} flight speed allows for a comparison to be made using data from both sites, and both particle size ranges (i.e., PM_{10} and $PM_{2.5}$) (Figure 5). Figure 5 shows clearly that the strength of the dust flux scales predictably and similarly as a function of speed, regardless of surface conditions and particle size range. This allows us to identify one of the key rotary-winged operating parameters that affects the dust emission process. Although we only had the opportunity to test one type of rotary-winged aircraft this type of relationship can be expected to hold for other single rotor blade helicopter models.

Based on these data we can propose a mechanism that explains, in part, this observed relationship. As the helicopter's forward speed increases its residence time over any location on the surface diminishes, so the time the downward rotor-generated flow is acting upon that surface must also decrease. As the revolutions per minute of the rotor is constant, the change in forward travel speed is a function of the pitch of the blade As the helicopter increases forward speed, the rotor blades change their pitch throughout the 360° rotation. The change in rotor blade pitch will alter the strength and distribution of the shear stresses created by the downward directed air flow from the rotor, which will also affect the dust emission process. The horizontal flux of sand and wind generated dust emissions scales with the shear stress generated by the wind (Shao, 2000), so we can assume that the magnitude of the rotor-created shear stresses should also affect dust emission strength.

4.3.2.2 Emissions during Landing and Takeoff

We had the opportunity to measure a series of three landings and four takeoffs at site 1. The emission flux expressed as kg-PM_{10} passing the flux plane for each event (landing or takeoff) is shown in Figure 6 with the average takeoff and landing emission fluxes superimposed on the graph.

These types of emission are basically from a point on the surface and are then lower in total mass emissions than the low-level flight tests. Based on the average values shown in Figure 6, a takeoff produced approximately 0.5 kg of PM_{10} and a landing

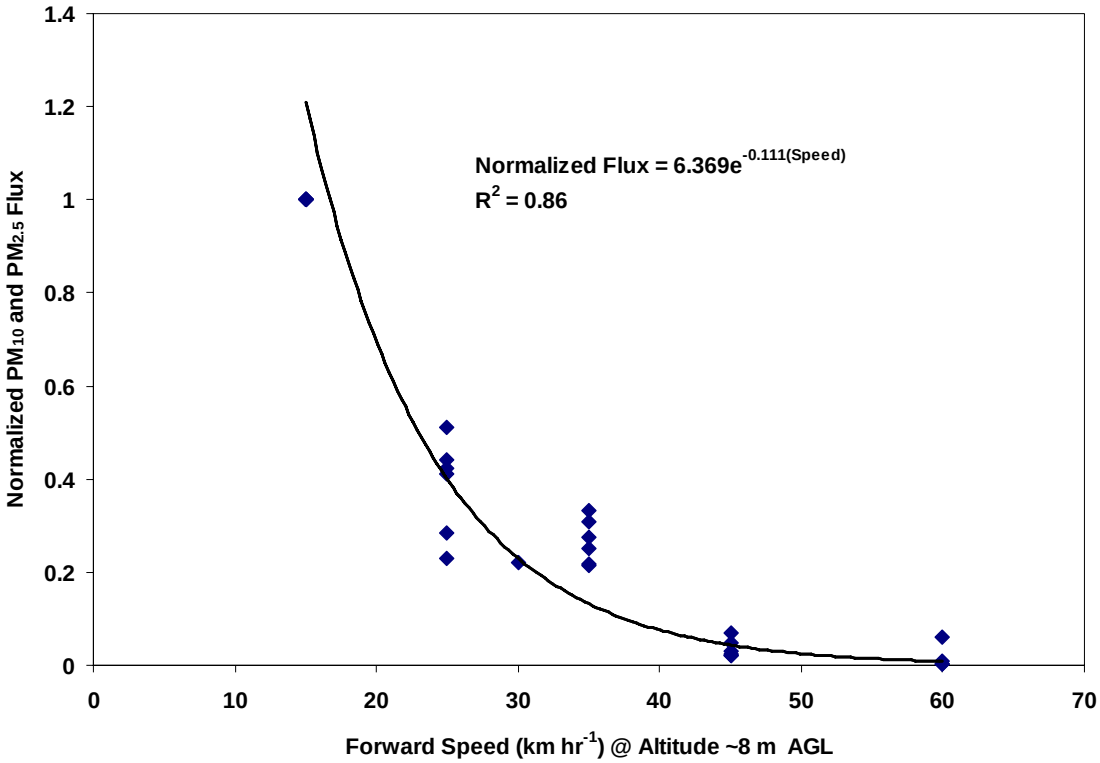

Figure 5. Normalized mean PM_{10} and $PM_{2.5}$ emission flux as a function of forward travel speed.

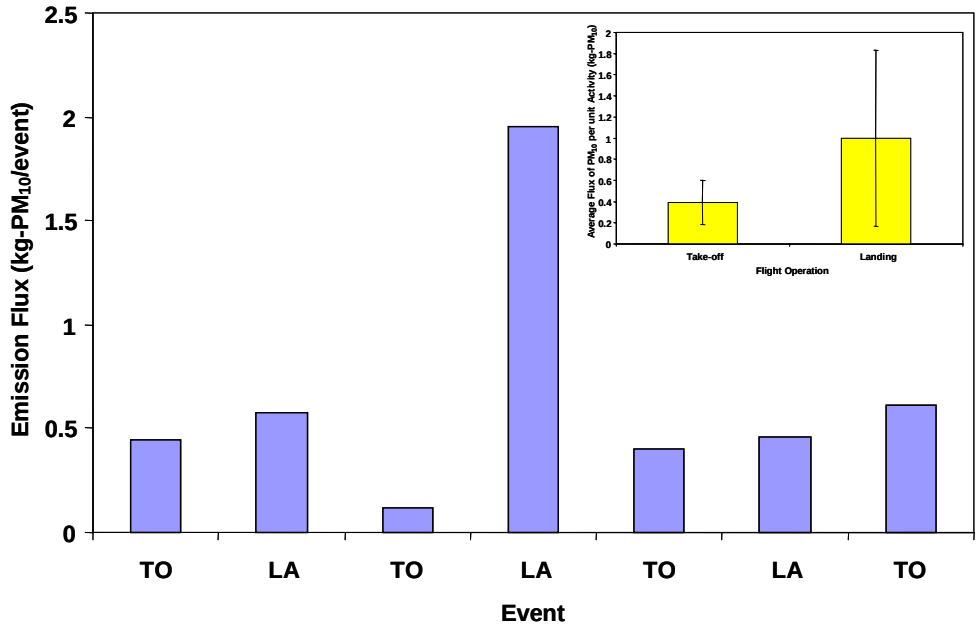

Figure 6. The emission fluxes measured for a series of takeoffs (TO) and landings (LA) measured at site 1. The graph in the upper right corner shows the mean and standard deviation of the takeoff and landing emission flux.

approximately 1 kg, or 2.5 times as much. This is explained by the longer time it takes to complete a landing than a takeoff so the surface experiences the force of the rotor downwash and the associated shear stresses for a proportionally longer time.

4.3.2.3 Surface Shear Stress Relationships

The Irwin sensors embedded in the surface allow for the evaluation of the strength and the pattern of the rotor-created shear stress. The Irwin sensor measures a delta pressure (Pa) between the surface and that measured at a height above that surface, but very close to the surface. Typically, and in our case as well, that height is 1.651 mm.

According to Irwin (1981), the delta pressure can be related to a shear stress using the following calibration relationship:

$$\frac{u_\tau h}{\nu} = 8.0 + 0.193\left(\frac{\Delta p h^2}{\rho}\right)^{0.453} \quad (1)$$

where: u_τ is skin friction velocity (m s^{-1}, note $u_\tau=(\rho_{air} \times \tau)^{0.5}$), h is the height above the surface of the second pressure measurement (i.e., 1.651 mm), ν is kinematic viscosity (m^2 s^{-1}), p is pressure (Pa), and ρ is fluid density (kg m^{-3}).

An example of the delta pressure data obtained from the four Irwin sensors is shown in Figure 7 for a helicopter pass at the forward travel speed of 15 km hr^{-1} at site 2. These data show that the Irwin closest to the flight line (10 m from the center line) experiences higher pressures than the one farthest away and the peak pressures occur later in time with increasing distance from the flight line. By aggregating the pressure data and converting it to a shear stress we can examine the relationships between aircraft forward speed and as a function of distance from the Irwin sensors.

Figure 8 shows the change in the mean peak shear stress measured at the same position for the range of forward travel speeds for site 2. For each increase in speed there is a decrease in the peak shear stress at each of the shear stress measurement locations. Normalizing each peak shear stress by dividing by the mean peak shear stress for the 15 km hr^{-1} speed, we can combine the data from sites 1 and 2 for the four Irwin sensors to define the speed effect on shear stress within ~19 m of the flight line. This relationship is shown in Figure 9 and it reveals that the shear stress changes proportionally the same amount at each measurement location for an incremental change in forward travel speed. At each of the Irwin sensor locations there is an ~0.05% decrease in mean peak shear stress for every 1 km hr^{-1} increase in forward travel speed. This decrease in shear stress at the surface as the flight speed increases adds an additional explanatory mechanism as to why dust emissions were observed to decrease as forward travel speed increases.

The Irwin sensor data can also be used to evaluate how the shear stress distribution changes as a function of distance from the flight line. The decrease in shear mean peak

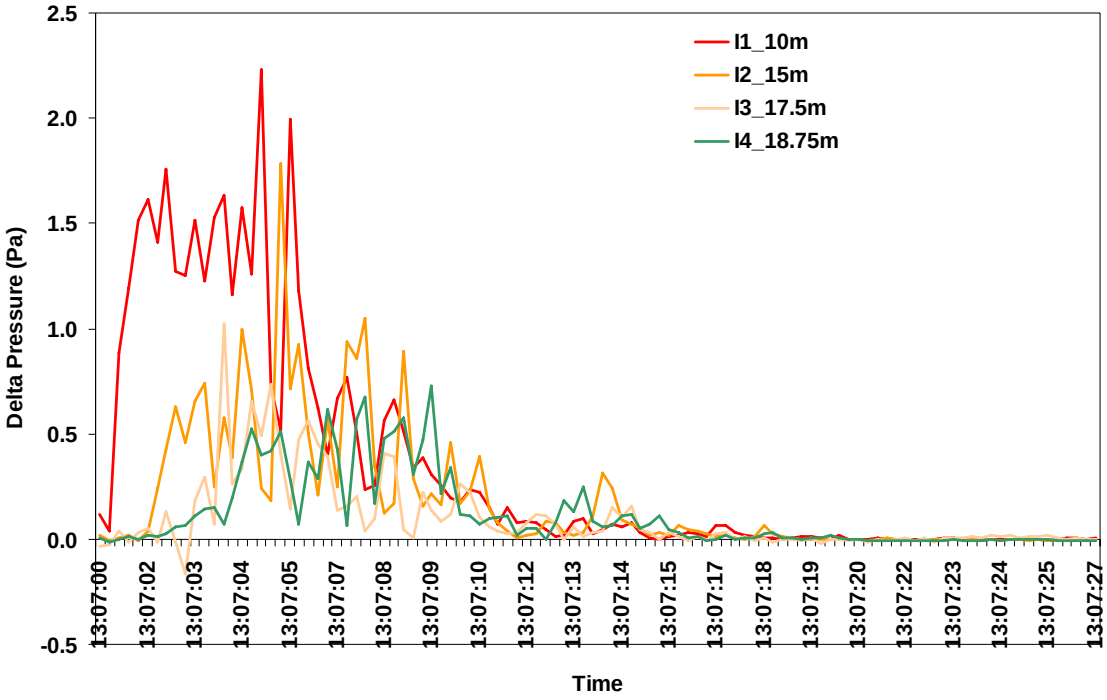

Figure 7. Time series of delta pressure associated with the passage of the aircraft traveling at 15 km hr^{-1} measured by the four embedded Irwin sensors. For this event the rotor-generated winds persist at the measurement points for approximately 19 seconds.

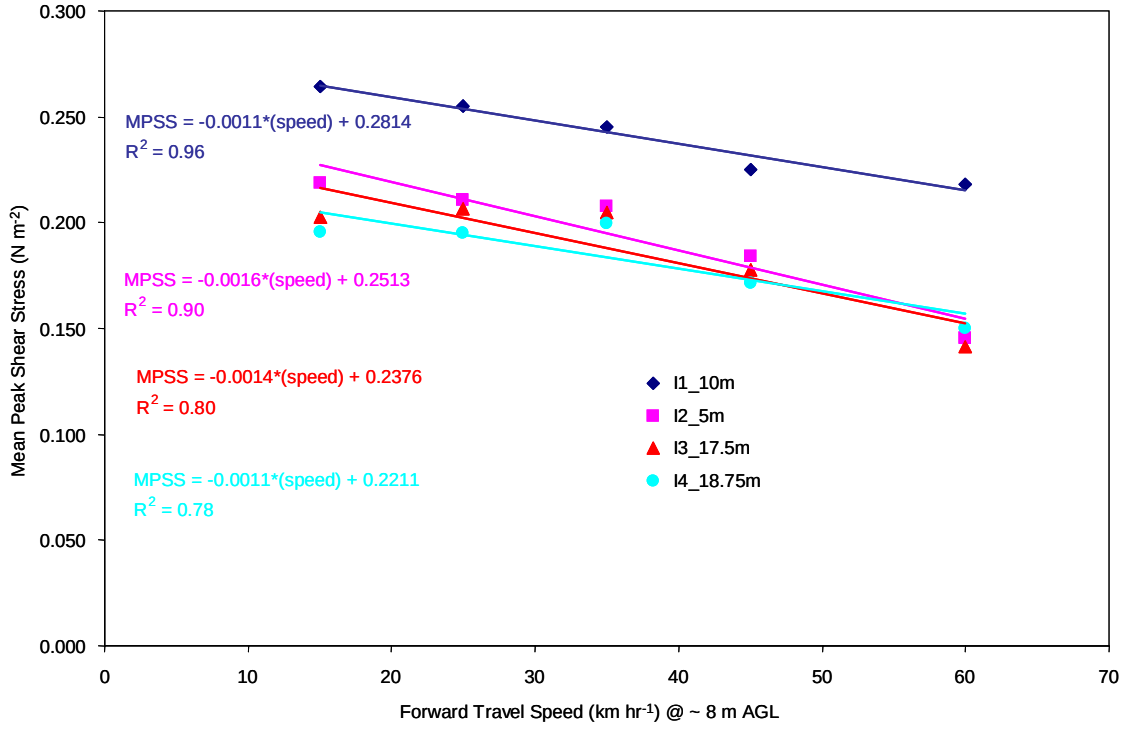

Figure 8. The change in mean peak shear stress at each Irwin sensor as a function of forward aircraft travel speed.

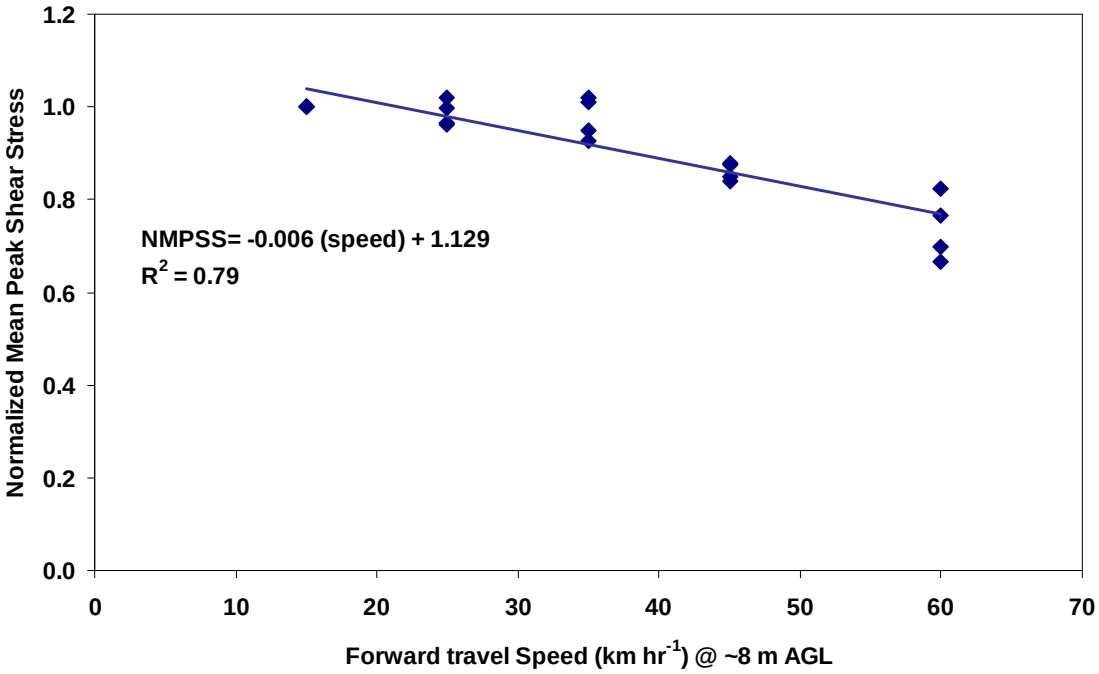

Figure 9. The change in normalized mean peak shear stress as a function of forward travel speed, 60 km hr^{-1} data are not included.

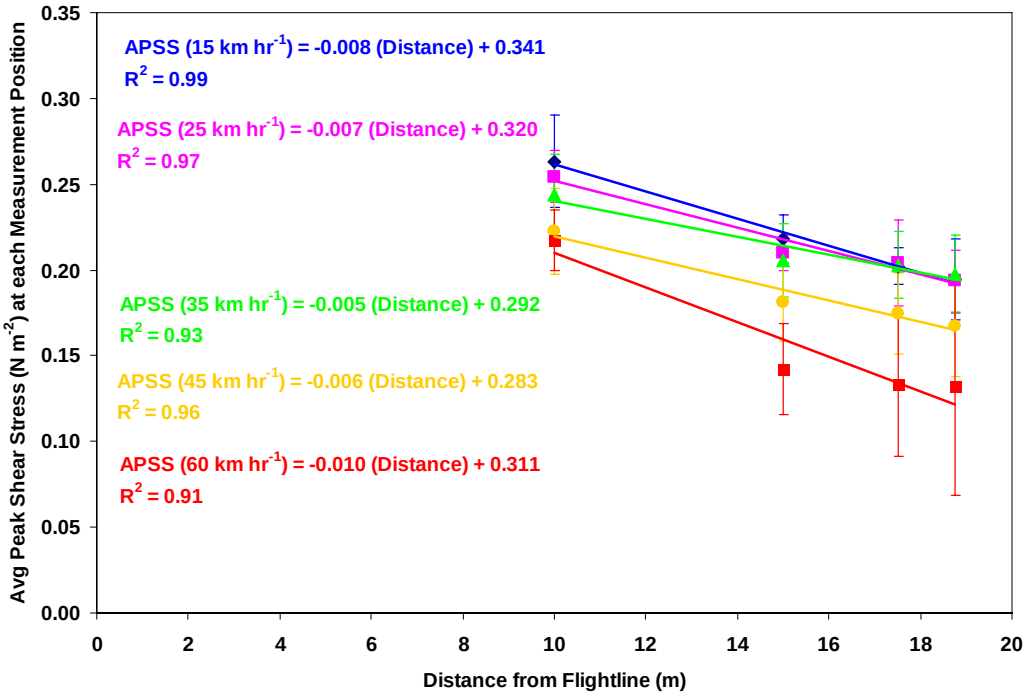

Figure 10. The change in mean peak shear stress as a function of distance from the flight line and for each of the five test speeds.

shear stress as a function of distance from the flight line and for each of the five test speeds is shown in Figure 10. If the data are normalized by dividing each by the mean peak shear stress measured at the first Irwin sensor (i.e., 10 m from the flight line center) the data for each travel speed can be compared, this is shown in Figure 11. Over the approximately ~9 m measurement distance the decay in shear stress appears to be best described by a linear function. For the speed range up to 45 km hr^{-1} the rate of change in the shear stress reduction as a function of distance appear to be quite similar, but for the 60 km hr^{-1} flight speed the shear stress decreases at a somewhat faster rate. The drop in shear stress for each m beyond 10 m from the flight line is 2.3% for the flight speeds ≤45 km hr^{-1} and 34% for the 60 km hr^{-1} speed tests.

The rate of decrease in peak shear stress as a function of distance from the centerline will define a zone around the helicopter where the dust is actively being emitted under the influence of the rotor-created outflow of wind. At some distance from the aircraft the shear stress will drop below the threshold for entrainment of sand and dust, similar to wind erosion processes. Although our data indicate a linear decrease over our measurement distance of ~9 m it is more likely that the decrease in shear stress is better described by an exponential function. However, for a first estimate of the zone of emission around the aircraft we can use the relationship defined in Figure 10 for aircraft flying ≤45 km hr^{-1}.

The PI-SWERL data show that at the lowest applied shear stress of 0.06 N m^{-2} dust emissions are generated at site 2. Making the assumption that this is near the threshold shear stress for dust emissions we can use this value to estimate at what distance from the aircraft the shear stress drops below threshold for each of the forward travel speeds. Over

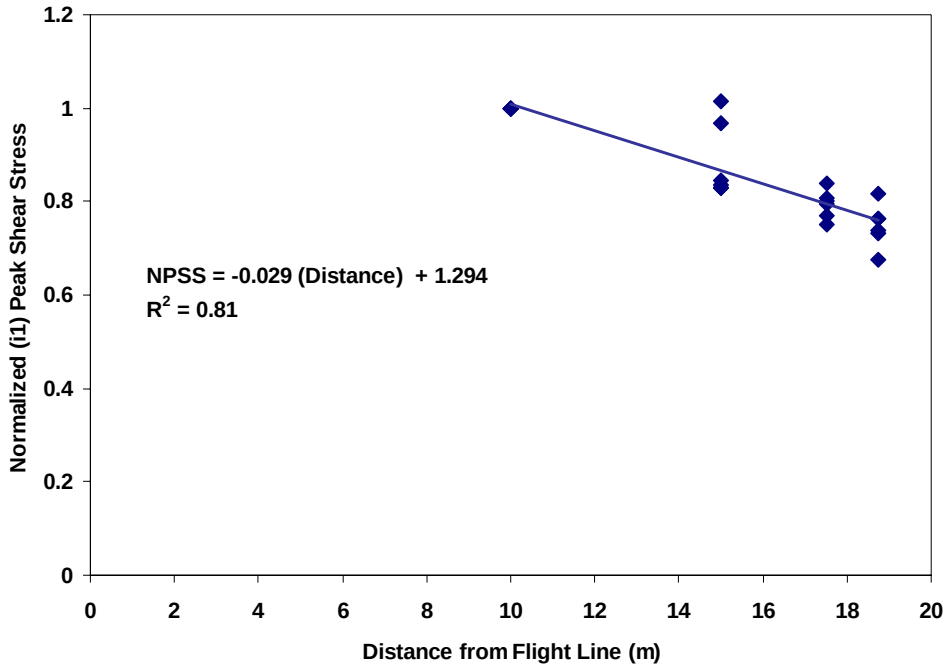

Figure 11. Normalized mean peak shear stress as a function of distance from the center of the flight line.

the range of speed from 15 km hr^{-1} to 45 km hr^{-1} the zone of shear that is ≥0.06 N m^{-2} can be defined as a circle of radius 39 m for the 15 km hr^{-1} and a radius of 32 m for the 45 km hr^{-1} travel speed. Beyond these distances the surface would not emit dust if we assume the threshold shear stress was 0.06 N m^{-2}. This demonstrates another factor that will tend to reduce the emissions of dust as the forward travel speed is increased.

These measurements have allowed us to begin to define how rotary-winged aircraft operating conditions affect the magnitude of the dust emissions they create. The three major factors identified from this study are: 1) as speed increases less time is spent over any point on the surface below the aircraft, 2) as speed increases the change in the rotor blade pitch directs less shear stress toward the surface, and 3) the decay of shear stress with distance from the center of the flight line creates a zone wherein the shear stress is above threshold for emissions, and this zone decreases in size as the applied shear stress becomes less, which could be a function of increasing travel speed or elevation of the aircraft above the surface.

This field campaign produced some of the most detailed dust emission and surface shear stress data available for a rotary-winged aircraft. These data will provide critical information to aid in a rotary-winged dust emission model. However, at the present time data have been collected for only one type of aircraft so the data are at this time applicable only to the aircraft we have measured. The rotor generated outflow from helicopters should scale with basically the weight of the aircraft as the downward force created by the rotor must be sufficient to keep the weight of the aircraft airborne. We plan to work with the DRI's Desert Terrain group who are developing a mechanistic dust emission model for rotary-winged aircraft to evaluate how the relationships developed for the UH-1H aircraft may scale for other types of single rotor blade military helicopters. The turbulence data that will be used to guide model development is discussed in a following section.

4.3.2.4 PI-SWERL Potential Emission Characterization

The PM_{10} emissions potentials were measured using the Portable In-Situ Wind Erosion Lab (PI-SWERL, Etyemezian et al., 2007; Sweeney et al., in press). The PI-SWERL is a VDC powered instrument that creates a shear stress on the surface within a cylindrical enclosure by a rotating annular blade within close proximity of the surface (Figure 12). It measures the PM_{10} concentration (C, mg/m^3) at an outlet with a DustTrak that records at 1 Hz while a blower vents clean air through the PI-SWERL at a constant rate (F, m^3 s^{-1}). By calibrating the PI-SWERL with the University of Guelph field wind-tunnel (Sweeney et al., in press) and from shear stress measurements made under the PI-SWERL in the laboratory this can be converted into an emission flux (mg m^2 s^{-1}) or amount of PM_{10} per area per second by:

$$E_{i,cum} = \frac{\sum_{begin,1}^{end,i} C \times F}{t_{end,i} - t_{begin,i}} \Big/ A_{eff} \qquad (2)$$

Where the summation occurs over every 1-second measurement during level i, beginning at $t_{begin,i}$ and ending at $t_{end,i}$, with t as integer seconds. The measured dust concentration and flow rate are converted to an emission flux by the effective area of the PI-SWERL,

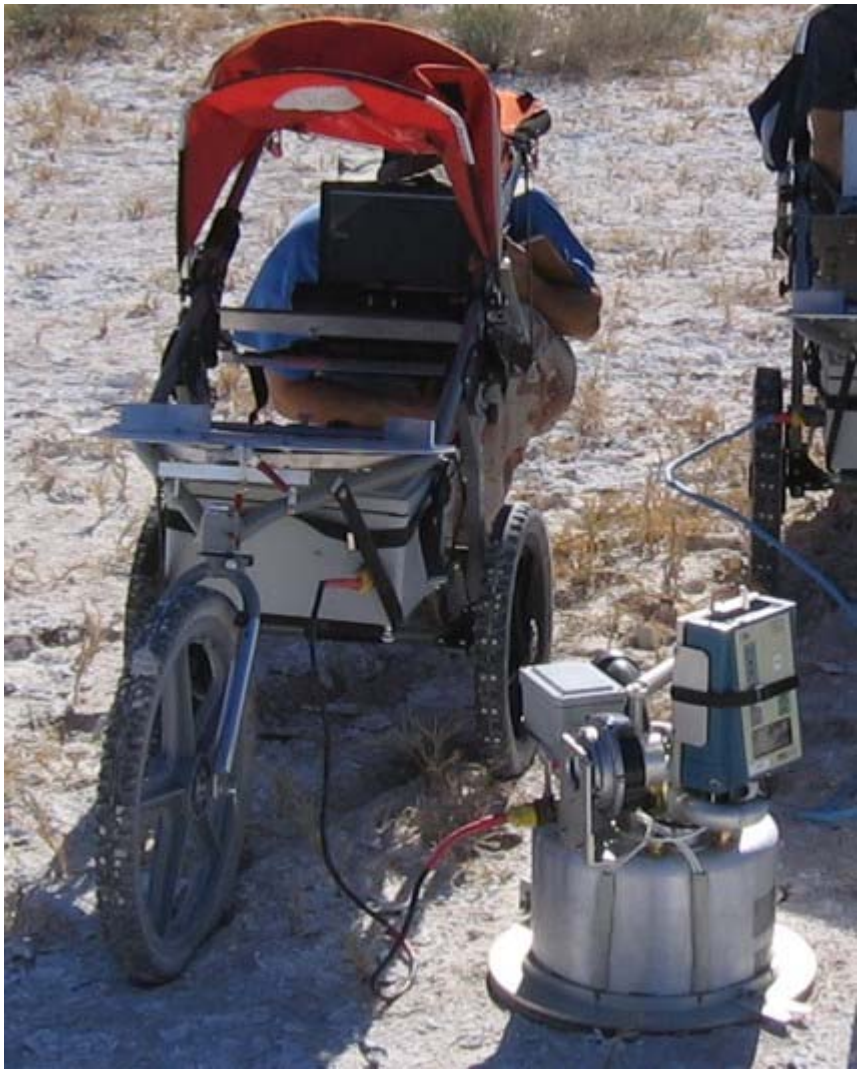

Figure 12. PI-SWERL in the field.

A_{eff} which is 0.07 m^2. A test sequence and the calculated E_i for each step increase in PI-SWERL speed and equivalent shear velocity (u_*) are shown in Figure 12 for a typical emission time series on an emissive surface. The PI-SWERL tests measure the potential fugitive PM_{10} dust emissions from the surface at different equivalent wind speeds. The tests are conducted at pre-set equivalent shear velocities that can go from 0.1 to 1.2 m s^{-1}, corresponding to a wind over 60 mph at pedestrian level.

PI-SWERL tests were conducted at each site before and after the helicopter passes. At each site multiple PI-SWERL tests were conducted on a parallel transect directly below where the helicopter flew over. At the first site 11 tests were conducted with 8 before the helicopter passes and 3 tests after the passes were completed. The second and third sites were at the same general location but on either side of a main access road and 17 tests were conducted in that area.

At site 1, the transect of PI-SWERL measurements produced equivalent shear velocities ranging from 0.23 to 0.81 m s^{-1} with the highest shear velocity generating PM_{10} dust

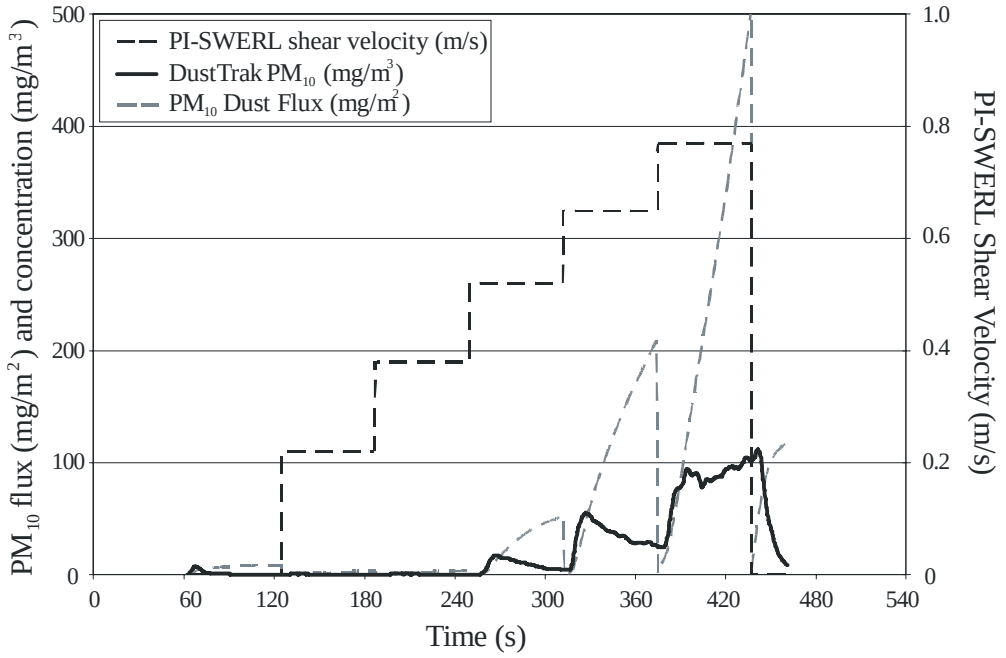

Figure 13. Example of PI-SWERL test showing typical response of a surface with increasing shear velocity

emissions that exceeded the limit (150 mg m^{-3}) of the dust monitor used (DustTrak, TSI Inc.). The dust flux from the surface exhibited an exponential relationship with shear velocity in almost cases shown in Figure 14 on a semi-logarithmic plot. The variability between tests is considerable with the standard deviation of the tests (pre- and post-helicopter passes) exceeding the geometric mean of the tests at each shear velocity interval. The range of PM_{10} emissions can be expressed by the geometric mean of all of the tests combined for shear velocities of 0.23, 0.39, 0.55, 0.69, and 0.81 m s^{-1}, which were 0.011, 0.060, 0.346, 2.168, 4.069 mg m^2 s^{-1}, respectively. The difference before and after the helicopter passes in dust emissions was not statistically significant but the emissions were higher on average for the same shear velocity for the PI-SWERL tests post-helicopter passes (e.g., for a shear velocity of 0.81 m s^{-1} the PM_{10} emissions were 2.86 and 6.87 mg m^2 s^{-1} for the pre and post-helicopter passes).

At the second site two different transects were measured at the same general location but on either side of a main access road. The PI-SWERL results reflect their close proximity to each other with no statistical difference between the PM_{10} emissions between sites, as well as pre-and post-helicopter passes. Equivalent shear velocities tested at these sites were as the first site but did not exceed 0.69 m s^{-1} (Figure 15) because of the PM_{10} measurement limits of the dust monitor and the very emissive surfaces.

At the location of the majority of test flight passes a set of eight tests were carried consisting of an inner transect line of three tests. The inner transect was conducted because of light winds and the subsequent request that the helicopter fly closer to the other instrumentation. Although the inner transect of PI-SWERL tests were conducted after the passing of the helicopter, no significant difference was found between the inner and outer sets of tests (Figure 16). The results from this site display a near exponential relationship between dust flux and shear velocity. This is because of an inflection point

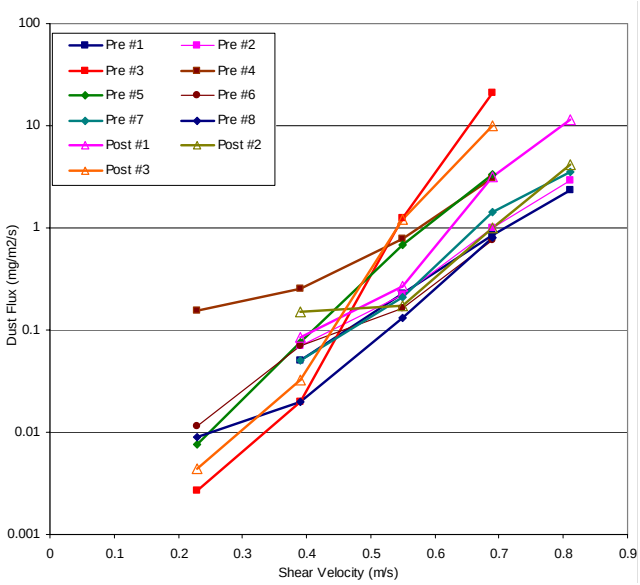

Figure 14. Site 1 PI-SWERL dust flux results.

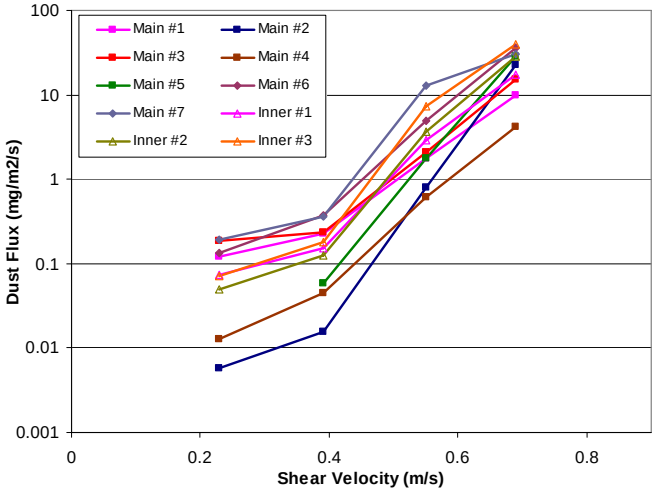

Figure 15. Site 2, transect 1 (primary flight line position) PI-SWERL dust flux results.

at a shear velocity of 0.55 m s^{-1} in the majority of the individual tests. The variability amongst the tests at this site is relatively large despite their similar trends resulting in a large standard deviation.

At the second transect at site 2, the PM_{10} emissions were not significantly different than those measured at the first transect (of site 2). At this position, a transect of six measurements were conducted to a maximum shear velocity of 0.69 m s^{-1} with one test over-ranging the PM_{10} monitor even at a shear velocity 0.69 m s (Figure 16).

On average the emissions from the second site (both transects) were an order of magnitude larger than at the first site for the same shear velocities (Figure 17). The surfaces at the

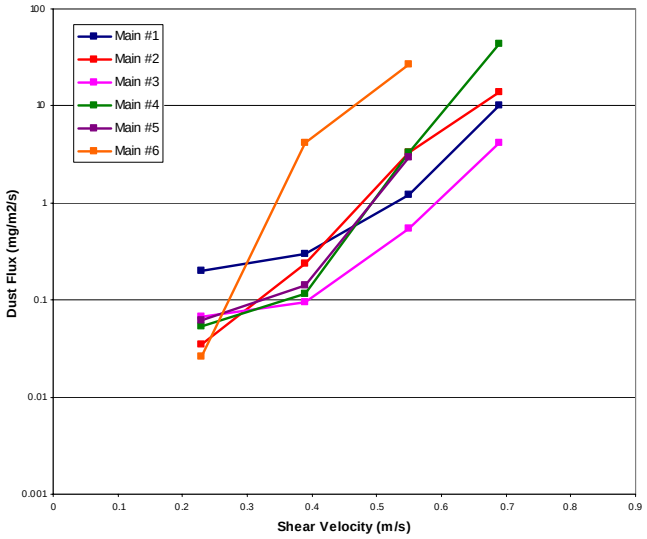

Figure 16. Site 2, transect 2 (secondary flight line position) PI-SWERL dust flux results.

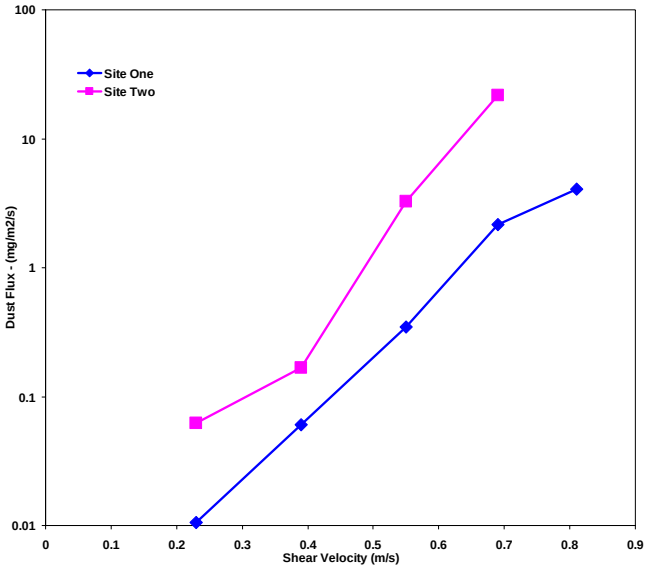

Figure 17. Average PI-SWERL dust emission fluxes for the same shear velocities for sites 1 and 2.

second site were very emissive and exhibited PM_{10} emissions beyond typical natural southwest desert surfaces.

4.4 ROTARY-WINGED AIRCRAFT TURBULENCE CHARACTERIZATION

The wind data collected by the sonic anemometer is key input in the development of the helicopter wake dust entrainment simulation. The data are pivotal in providing a source of validation for the modeling effort in terms of the flow field in the helicopter wake and the associated turbulent flux. The sonic wind data has been used so far to develop several products used for the modeling and visualization effort and will be used extensively through the next modeling development and analysis stages.

Sonic wind data was collected on Day 1 and Day 3 of the experiment. Background wind data were collected for a half-hour period before the first helicopter pass for analysis of background atmospheric conditions. Background wind data directly before and after each pass were also important to characterize the changing atmospheric conditions during the helicopter pass. This background data was used to estimate the plume dimensions for visibility analysis (McAlpine et. al., 2007).

Each helicopter pass over the sonic anemometer resulted in a time series of wind information. The time series of vertical and horizontal wind components and wind direction were plotted in relation to the relative distance of the helicopter from the sonic anemometer in time. These time series have provided insight into the structure of the helicopter wake at different helicopter pass speeds and background wind conditions. Further analysis of these time-series will be conducted to estimate wake dimensions for comparison to helicopter wake theory discussed in the literature. The wake characteristics will also be compared to the shear stress data collected by the Irwin sensors.

The degree of wind velocity considerably varied in the vertical and horizontal depending on the background wind speed and direction. Likely this is due to the interaction of the wake with the wind field and the position of the rotor-induced jet in relation to the sonic anemometer. The extreme vertical velocities measured were on the order of 20 m s^{-1} during the 15 and 25 km hr^{-1} passes. This is in comparison to maximum vertical velocities on the order of 8 to 10 m s^{-1} during the faster 45 and 60 km hr^{-1} passes. Maximum horizontal winds were on the order of 25-30 m s^{-1} for the slower 15 and 25 km hr^{-1} passes and on the order of 15-20 m s^{-1} for the faster 45 and 60 km hr^{-1} passes. The increase in velocities with lower helicopter speed lead to more wind forcing at the surface and as a result more shear stress and more dust emission. This was evident qualitatively as much more dust was emitted during slower passes.

The duration of maximum wind impact varies also with helicopter speed. Slower passes (15 and 25 km hr^{-1} passes) had pulses of vertical winds > 3 m s^{-1} for an average of 3 seconds while the fastest speeds (60 km hr^{-1} passes) had vertical velocities >3 m s^{-1} for an average of 0.5 seconds. An example of a time-series from a 25 km hr^{-1} pass (pass No. 34 on Day 3 with background wind speed at 6 m s^{-1}, wind direction: -1° from normal to the flight course) is included in the following Figure 17.

Spectral analysis of the wind data during the helicopter pass was conducted as a method to explore the turbulent flux within the helicopter wake. Analysis was conducted on the wake for two periods of each pass: while the helicopter was directly over the sonic anemometer and after the passing of the helicopter. Analysis during the overhead period is used to find the characteristics of tip vortex shedding. Analysis of the later period is used to characterize the wake shedding frequency. Both of these phenomena play a significant role in the variance of shear stress at the surface due to the wake, and therefore are important to understand to characterize the dust entrainment. The characteristic turbulent periods calculated are now being compared to theory found in the literature and will be used to verify the fluid modeling of the helicopter wake.

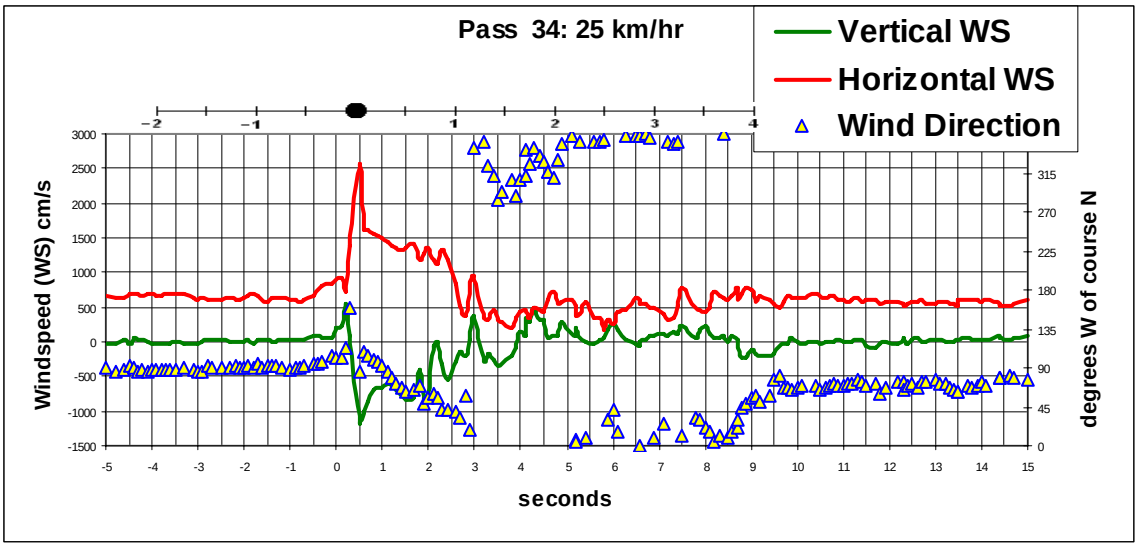

Figure 17. Time series of a pass of the helicopter traveling at 25 km hr^{-1}. Wind direction is in degrees west of course north (helicopter flew along line from "course south" to "course north," and vertical and horizontal wind speed is plotted in cm s^{-1}. A helicopter rotor position indicator bar is included at the top of the graph: the black dot represents the moment that the rotor center was directly over the sonic anemometer as verified by the video data. The numbers on the bar represent a rotor diameter of distance from the sonic anemometer (example: "-2" indicates that the center of the helicopter rotor is 2 rotor diameters in distance from the sonic anemometer).

Spectral analysis of the wind data during the helicopter pass was conducted as a method to explore the turbulent flux within the helicopter wake. Analysis was conducted on the wake for two periods of each pass: while the helicopter was directly over the sonic anemometer and after the passing of the helicopter. Analysis during the overhead period is used to find the characteristics of tip vortex shedding. Analysis of the later period is used to characterize the wake shedding frequency. Both of these phenomena play a significant role in the variance of shear stress at the surface due to the wake, and therefore are important to understand to characterize the dust entrainment. The characteristic turbulent periods calculated are now being compared to theory found in the literature and will be used to verify the fluid modeling of the helicopter wake.

4.5 Dust Emissions and Visibility in the Vicinity of Flight Operations

The DRI, Desert Terrain Project, is also using the dust emission and environmental variables collected to aid in developing a treatment to simulate the visibility degradation associated with dust emissions from rotary-winged aircraft for computer visualization purposes and eventual simulation. A citation and the associated abstract from work published in 2007 is provided below.

McAlpine, J.D., D. Koracin, K. Veropoulos, D. Boyle, E. McDonald, and G. Lamorey (2007). Determining atmospheric dust concentrations during strong flow perturbations using a digital-optical technique. *Lecture Notes in Computer Science: Advances in Visual Computing*, **4841**, 393-402.

Dust emissions due to low-level flight of a helicopter are studied as part of the Integrated Desert Terrain Forecasting for Military Operations project. Atmospheric concentrations of PM_{10} were measured at different heights downwind of the helicopter flight path. Digital video images captured the entrainment and dispersion of the dust plume formed by the wake of the helicopter during each pass down the flight course. The video data are analyzed to relate the dust plume strength to degradation of local visibility. A strong relationship between color changes/standard deviations and plume strength is found. This relationship is used to develop an algorithm that can determine local visibility degradation due to local PM_{10} concentrations around a helicopter. This algorithm can be combined with concentration output data from an atmospheric dispersion model to simulate visibility in a helicopter simulator.

4.6. CHARACTERIZATION OF SURFACE DUST EMISSION POTENTIAL: DRI PI-SWERL

As PI-SWERL is an important part of our SERDP research project for characterizing the emission potential of surfaces that unique military activities and vehicles may create emissions on, we feel it is important to keep SERDP apprised of its research applications and the publications that document its use. In 2007 one manuscript was published and another is in press. The citations and the paper abstracts follow:

Etyemezian, V., G. Nikolich, S. Ahonen, M. Pitchford, M. Sweeney, J. Gillies, and H. Kuhns (2007). The Portable In-Situ Wind Erosion Laboratory (PI-SWERL): a new method to measure PM_{10} windblown dust properties and potential for emissions. *Atmospheric Environment* **41**: 3789-3796.

A new device—the Portable In Situ Wind ERosion Lab (PI-SWERL)—for measuring the potential for wind erosion and dust emission from soil surfaces is described. The device uses an annular ring (inner diameter ¼ 39 cm, outer diameter ¼ 51 cm) that rotates 6 cm above the soil test surface. Dust and sand are mobilized by the shear created by the rotating ring. Dust concentrations within the chamber that encloses the annular ring are measured by light scattering, used as a surrogate for particulate matter mass concentrations. While the PI-SWERL does not realistically simulate natural wind erosion processes that are often driven by saltation, measurements with the device provide a robust index of wind erosion/dust emission potential. Compared to traditional field wind tunnels used for the same purpose, the PI-SWERL offers significant economy in size, portability, and ease of use.

Sweeney, M., V. Etyemezian, T. Macpherson, W. Nickling, J. Gillies, G. Nikolich, and E. McDonald (2007). Comparison of PI-SWERL with dust emission measurements from a straight-line field wind tunnel. *Journal of Geophysical Research, Earth Surface* (in press).

The Portable *In Situ* Wind ERosion Lab (PI-SWERL) was developed to measure dust emissions from soil surfaces. This small, portable unit can test the emissivity of soils in areas that are difficult to access with a field wind tunnel, and can complete a larger number of tests in less time. The PI-SWERL consists of a cylindrical enclosure containing an annular flat blade that rotates at different speeds, which generates shear stress upon the surface. The shear stress generated by PI-SWERL results in the entrainment of particles including dust. PI-SWERL was developed to provide an index

of dust emission potential comparable to the field wind tunnel. The PI-SWERL dust emission results were compared against those obtained from a ~12 m long, 1 m wide, 0.75 m high straight line suction-type portable field wind tunnel by conducting collocated tests at 32 distinct field settings and soil conditions in the Mojave Desert of southern California. Clay- to sand-rich soils that displayed a range of crusting, gravel cover, and disturbance were tested. The correspondence between dust emissions (mg m^2 s^{-1}) for the two instruments is nearly 1:1 on most surfaces. Deviation between the two instruments was noted for densely packed gravel surfaces. For rough surfaces a correction can be applied to the PI-SWERL that results in comparable dust emission data to the wind tunnel. PI-SWERL can be used to complement research efforts in aeolian geomorphology aimed to quantify spatial and temporal patterns of dust emissions as well as air quality research related to dust emissions.

4.7 DUSTRAN

PNNL activities involving the atmospheric dispersion modeling system DUSTRAN during calendar year 2007 on the SERDP Unique Dust Emissions Project SI-1399 focused on further improving the already substantial user-friendliness of DUSTRAN in addition to accommodating artillery backblast and tank activities as dust sources. Highlights include the following:

- Initial development on DUSTRAN to add a new tab under the point source input window to include the dust emission factors from artillery backblast. Based upon the input form used for wheeled vehicles, this new tab will allows users the ability to enter input data for artillery activities including times fired, zone charge, and bore size. Initial modifications have also taken place on the vehicle tab to include the ability to select tracked vehicles such as the M1A1 Abrams as well as the current wheeled vehicles. New data displayed as input in the window will include information concerning the tracks of the vehicles such as track width and pad length and pad width.

- Two modules to provide automated checks and conditioning of input meteorological data required for DUSTRAN simulations were developed, tested, and integrated into the DUSTRAN system. The CALMET meteorological model of DUSTRAN requires certain surface and upper air information in a specific input format, the surf.dat and up.dat files, respectively. DUSTRAN automatically generates these CALMET-required files from either user-specified meteorological information or from National Weather Service data captured using the MetArchiver tool, a DUSTRAN utility developed in 2006. Now two new FORTRAN-based executables, “SURFCheck” and “UPCheck,” perform a series of range checks against the meteorological data as well as ensuring that all of the required upper-air and surface observations are present. These checks are particularly important when real-time meteorological data are being used. The two new modules serve to make DUSTRAN even more user-friendly by preventing the sudden termination of DUSTRAN simulations due to missing or erroneous meteorological data.

- The DUSTRAN modeling system and interface were modified to allow a user the ability to specify many point-source locations via a file (XML text) rather than just specifying by graphical means through DUSTRAN maps. The source file is read and

automatically adds the sources to an ongoing simulation as well as creating a default "unit" release for each of the source locations. With the unit release specified for each source, DUSTRAN can be immediately run displaying the plume footprint of potential emissions from these points. This modification improves the user-friendliness of the DUSTRAN system by automating a potentially time-consuming user-input task. Graphical output was also modified to allow the display of simulation results from the different sources in varying colors, permitting easy identification of which sources are most directly impacting a particular receptor region.

- The MetArchiver tool, a utility developed in 2006 to automate the tasks of locating and preparing either historical or real-time meteorological data for DUSTRAN simulations, underwent several modifications and improvements. The tool was originally developed to obtain upper-air and surface meteorological data from the National Oceanic and Atmospheric Administration's websites and store these data in a local database. This year the MetArchiver application and database were modified to allow the downloading and processing of data from localized meteorological networks, greatly increasing the number of potential sources for real-time meteorological information. The database file used by the MetArchiver application was expanded to include more station-specific information as well as more types of meteorological data. The expanded database file includes time zone, station elevation, anemometer height, and standard deviation of wind speed and direction. Additionally, a "station characteristics" file now can be used to import information on upper air and surface stations into the MetArchiver tool. This file contains a list of stations and their characteristics, such station identification, latitude, longitude, elevation, and anemometer height, and, as a comma separated text file, is extremely easy for a user to generate. Lastly, the MetArchiver tool was modified to allow the import and export of the upper-air and surface station name files (UNF and SNF) used by the DUSTRAN modeling system. With this modification, the system now automatically creates the meteorological station files required by DUSTRAN for a new simulation site as well as automatically updating the MetArchiver station fields for existing site station files. All of these changes together serve to improve and expand the user-friendliness of both the MetArchiver utility and the overall DUSTRAN system.

- It was discovered that wind vectors displayed at meteorological station locations were not being scaled in the same manner as the wind vector fields created by the CALMET model. Although this situation did not affect winds used in dispersion routines and thus did not affect predicted concentrations, scaling was modified so that all displayed wind vectors are scaled in a consistent manner throughout the modeling domain.

Although not funded directly under SI-1399, four additional activities related to the scientific and public dissemination of DUSTRAN deserve mention. First, a manuscript entitled "An evaluation of the wind erosion module in DUSTRAN" by W.J. Shaw, K.J. Allwine, B.G. Fritz, F.C. Rutz, J.P. Rishel and E.G. Chapman was accepted for publication in the scientific journal *Atmospheric Environment*. The article focuses on the scientific underpinnings of the wind erosion source term in DUSTRAN and comparison

of DUSTRAN-derived PM_{10} concentrations with observations (Shaw et al., 2007). Second, the DUSTRAN modeling system was the subject of an invited oral presentation at the 2007 Annual Meeting of the Emergency Management Issues - Special Interest Group (EMI-SIG). The presentation focused on a description of DUSTRAN and its potential for use as an emergency response tool (Rishel and Allwine, 2007). Third, the final technical report on the development of DUSTRAN was submitted to SERDP and published as a PNNL report (Allwine et al., 2007). Fourth, because of wide-spread interest in DUSTRAN, development was initiated on a website describing the DUSTRAN and SPRAYTRAN modeling systems and providing links to open literature publications. It is expected that the website will become publicly available in 2008.

The citation and abstract for this in press paper follow:

Shaw, W.J., K.J. Allwine, B.G. Fritz, F.C. Rutz, J.P. Rishel, and E.G. Chapman (2007) An evaluation of the Wind Erosion Module in DUSTRAN. *Atmospheric Environment*, doi:10.1016/j.atmosenv.2007.11.022

Pacific Northwest National Laboratory (PNNL) has developed a dust transport model (DUSTRAN), which calculates atmospheric dust concentrations that result from both natural and human activity. DUSTRAN is a comprehensive dispersion modeling system, consisting of a dust-emissions module, a diagnostic meteorological model, and dispersion models that are integrated seamlessly into graphical information system (GIS) software. DUSTRAN functions as a console application and allows the user to interactively create a release scenario and run the underlying models. We have recently compared dust concentrations calculated by DUSTRAN with observations of wind erosion on the US Department of Energy's Hanford Site in southeastern Washington. In this paper we describe both DUSTRAN's algorithm for predicting the source strength of wind-blown dust and the comparison of simulated dust concentrations with data. The comparisons use observations of PM10 concentrations for three separate dust events on the Hanford Site in 2001. The dust measurements were made as part of an effort to monitor site recovery following a large range fire that occurred in 2000. The comparisons have provided both encouragement as to the practical value of the wind erosion module in DUSTRAN and examples of occasions when the simulations and observations diverge. In general, the maximum dust concentrations from the simulations and the observations for each dust event agreed closely. Because of the lack of soil moisture information, the model was run in a ''dry'' mode. However, certain discrepancies between the measured and simulated values relative to the timing of observed precipitation events suggest that soil moisture should be accounted for where possible. For low dust concentrations, DUSTRAN tends to overestimate PM_{10} levels. This may be a weakness in the form of the dust flux parameterization at low wind speeds. Overall, however, we have shown DUSTRAN to be an effective tool for simulating dust events due to wind erosion.

5. REFERENCES

Chow, J.C., J.G. Watson, J.E. Houck, and L.C. Pritchett (1994). A laboratory resuspension chamber to measure fugitive dust size distributions and chemical compositions. *Atmospheric Environment*, **28**(21): 3463-3481.

Etyemezian, V., G. Nikolich, S. Ahonen, M. Pitchford, M. Sweeney, J. Gillies, and H. Kuhns (2007). The Portable In-Situ Wind Erosion Laboratory (PI-SWERL): a new method to measure PM_{10} windblown dust properties and potential for emissions. *Atmospheric Environment* **41**: 3789-3796.

Gillies , J.A., V. Etyemezian, H. Kuhns, J. Engelbrecht, S. Uppapalli, and G. Nikolich (2007a). Particulate emissions from U.S. Department of Defense artillery backblast testing. *Journal of the Air & Waste Management Association*, **57**: 551-560.

Gillies, J.A., V. Etyemezian, H. Kuhns, D. Nikolic, and D.A. Gillette (2005). Effect of vehicle characteristics on unpaved road dust emissions. *Atmos. Environ.*, **39**: 2341–2347.

Gillies, J.A., W.G. Nickling, and J. King (2006). Aeolian sediment transport through large patches of roughness in the atmospheric inertial sublayer. Journal of Geophysical Research - Earth Surface, 111(F02006): doi:10.1029/2005JF000434.

Gillies, J.A., W.G. Nickling, and J. King (2007). Shear stress partitioning in large patches of roughness in the atmospheric inertial sublayer. *Boundary-Layer Meteorology*, **122** (2), doi: 10.1007/s10546-006-9101-5, 367-396.

Irwin, H.P. (1981). A simple omnidirectional sensor for wind tunnel studies of pedestrian level winds. *Journal of Wind Engineering and Industrial Aerodynamics* **7** (3): 219-239.

Shao, Y. (2000). *Physics and Modelling of Wind Erosion*. Kluwer Academic Publishers, Dordrecht, 393 pp.

Shaw, W.J., K.J. Allwine, B.G. Fritz, F.C. Rutz, J.P. Rishel, and E.G. Chapman (2007) An evaluation of the Wind Erosion Module in DUSTRAN. *Atmospheric Environment*, doi:10.1016/j.atmosenv.2007.11.022 (in press).

Sweeney, M., V. Etyemezian, T. Macpherson, W. Nickling, J. Gillies, G. Nikolich, and E. McDonald (2007). Comparison of PI-SWERL with dust emission measurements from a straight-line field wind tunnel. *Journal of Geophysical Research, Earth Surface* (in press).

APPENDIX A

PUBLISHED TECHNICAL ABSTRACTS

SERDP Annual Symposium, Washington, D.C., Dec. 3-6, 2007.

PARTICULATE MATTER EMISSIONS FOR DUST FROM UNIQUE MILITARY ACTIVITIES: ROTARY-WINGED AIRCRAFT

John A. Gillies, Ph.D.
Desert Research Institute
2215 Raggio Parkway
Reno, NV, 89512
775-674-7035
jackg@dri.edu

Co-Performers: V. Etyemezian, Ph.D.; H. Kuhns, Ph.D.; H. Moosmüller, Ph.D.; J. Engelbrecht, Ph.D.; J. King, Ph.D.; M Skiba, Ph.D., J.D. McAlpine; .D.A. Gillette, Ph.D.; R. J. Allwine, Ph.D; R. Hashmonay; PhD.

Dust emissions are created by activities often unique to the testing and training activities of the DoD. As part of SERDP Project SI-1399, emissions of dust raised by rotary-winged aircraft activities were measured at the Yuma Proving Ground (YPG), Yuma AZ, in May 2007. Dust emissions measurements, from which emission factors can be developed, were carried out with a three-tower system and in conjunction with optical remote sensing measurements made by SERDP Project SI-1400. Each of the towers is equipped with instruments to measure the vertical concentration of dust in the emitted plumes at 1 Hz. One of the three towers is also instrumented with cup anemometers to measure the vertical wind speed profile and a wind vane to measure wind direction. The meteorological measurements are combined with the dust concentration measurements to estimate the unit flux of dust emissions for each activity. The use of three towers allows better characterization of the emitted dust plumes in the vertical and horizontal planes and better estimation of emission fluxes than single point measurements. The strength of the rotor downwash and the shear stress created by the downwash as it travels laterally across the surface were measured with a sonic anemometer and Irwin sensors. Measurements of the emission potential of the surface and the threshold shear stress at which dust is entrained were also made using the DRI PI-SWERL instrument. The suspended dust was collected using filter samplers to develop representative samples of its chemical and mineralogical composition for this area.

The dust emissions were created by a UH-1H Huey traveling above two different desert surface types over a range of speeds with the rotor blade at the same height above the surface (8 m) for each test. In addition, dust emissions were measured for several landing and takeoff sequences as well as hovering maneuvers. The strength of the emission was observed to scale negatively with aircraft forward speed. This occurs for two reasons: 1) as the forward speed is increased more thrust is directed to the rear of the aircraft due to change in blade pitch, and 2) as aircraft speed increases the residence time per unit of travel distance is decreased. The dust emission measurements for the UH-1H aircraft and estimated emission factors for the activities tested will be included as part of this poster presentation..

ARTICLES AND PAPERS IN PEER-REVIEWED PUBLICATIONS

Etyemezian, V., G. Nikolich, S. Ahonen, M. Pitchford, M. Sweeney, J. Gillies, and H. Kuhns (2007). The Portable In-Situ Wind Erosion Laboratory (PI-SWERL): a new method to measure PM_{10} windblown dust properties and potential for emissions. *Atmospheric Environment* **41**: 3789-3796.

Gillies, J.A., V. Etyemezian, H. Kuhns, J. Engelbrecht, S. Uppapalli, and G. Nikolich (2007). Dust emissions caused by backblast from Department of Defense artillery testing. *Journal of the Air & Waste Management Association* **57**, doi:10.3155/1047-3289.57.5.551, 551–560.

Sweeney, M., V. Etyemezian, T. Macpherson, W. Nickling, J. Gillies, G. Nikolich, and E. McDonald (2007). Comparison of PI-SWERL with dust emission measurements from a straight-line field wind tunnel. *Journal of Geophysical Research, Earth Surface* (accepted for publication).